Role of ammonia on fine-particle pH in agricultural regions of China: Comparison between urban and rural sites

Shenbo Wang [a], Lingling Wang [b], Yuqing Li [c], Chen Wang [a], Weisi Wang [b], Shasha Yin [a, *], Ruiqin Zhang [a, *]

[a] *Research Institute of Environmental Science, College of Chemistry, Zhengzhou University, Zhengzhou, 450001, China*

[b] *Department of Environmental Protection of Henan Province, Zhengzhou, 450001, China*

[c] *Department of Environment Science and Engineering, Tsinghua University, Beijing 100084, China*

Text S1 Calculation of ions balance and equivalent ratio.

Fig. S1 Ion balance of water-soluble inorganic ions at five sites (i.e., urban sites at Zhengzhou (U-ZZ) and Anyang (U-AY), rural sites at Anyang (R-AY), Xinxiang (R-XX), and Puyang (R-PY)).

Fig. S2 Comparisons of predicted and measured NH_4^+, SO_4^{2-}, NO_3^-, NH_3, HNO_3 and HCl at the five sites.

Fig. S3 Comparison of predicted pH by ISORROPIA-II with E-AIM IV at U-ZZ site.

Fig. S4 Fig. 2 Temporal variations of temperature (T), relative humidity (RH), wind speed (WS), wind direction (WD), and concentrations of NH_3 and water-soluble inorganic ions (WSIIs) in three cases at U-AY (a), R-AY (b), R-XX (c), and R-PY (d) sites.

Fig. S5 Trajectory frequencies of typical periods during Cases 1 (a), 2(b), and 3 (c).

Fig. S6 Sensitivity tests of $PM_{2.5}$ pH to Na^+, K^+, Ca^{2+} and Mg^{2+} in Case 2. The color scale bar represents the pH values. The relative standard deviation (RSD) and range (Range) represent the variation degree and range of pH values in the test.

Table S1 Summarized of NH_3 concentrations in this study and other sites.

Table S2 Pearson's correlation coefficients (r) between H^+_{air} and input data at the five sites.

Text S1 Calculation of ions balance and equivalent ratio.

The ions balance and equivalent ratio are calculated using following formulas:

$$[\text{cations}] = \frac{[NH_4^+]}{18} + \frac{[Na^+]}{23} + \frac{[K^+]}{39} + \frac{[Ca^{2+}]}{20} + \frac{[Mg^{2+}]}{12} \quad (1)$$

$$[\text{anions}] = \frac{[SO_4^{2-}]}{48} + \frac{[NO_3^-]}{62} + \frac{[Cl^-]}{35.5} \quad (2)$$

$$\text{ion balance} = [\text{cations}] - [\text{anions}] \quad (3)$$

$$\text{equivalent ratio} = [\text{cations}]/[\text{anions}] \quad (4)$$

where $[Na^+]$, $[K^+]$, $[Ca^{2+}]$, $[Mg^{2+}]$, $[NH_4^+]$, $[SO_4^{2-}]$, $[NO_3^-]$, and $[Cl^-]$ are the measured concentrations ($\mu g/m^3$) in the atmosphere. The results presented in Fig. S1 show that the observed water-soluble inorganic ions have good balance and are effective as input data for ISORROPIA-II model. In addition, the equivalent ratio suggest that particle was acidic at U-ZZ site and alkaline at other four sites.

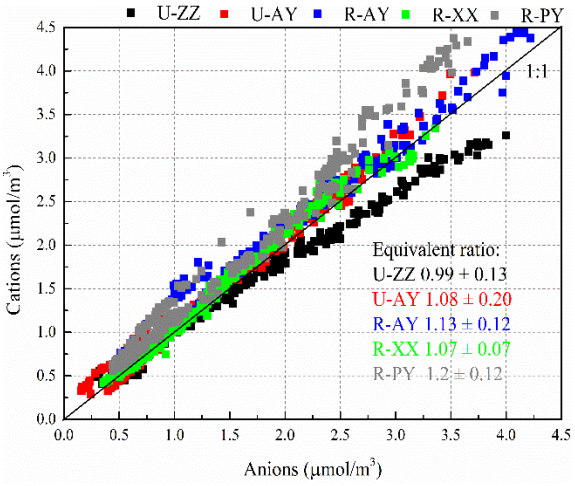

Fig. S1 Ion balance of water-soluble inorganic ions at five sites (i.e., urban sites at Zhengzhou (U-ZZ) and Anyang (U-AY), rural sites at Anyang (R-AY), Xinxiang (R-XX), and Puyang (R-PY)).

.

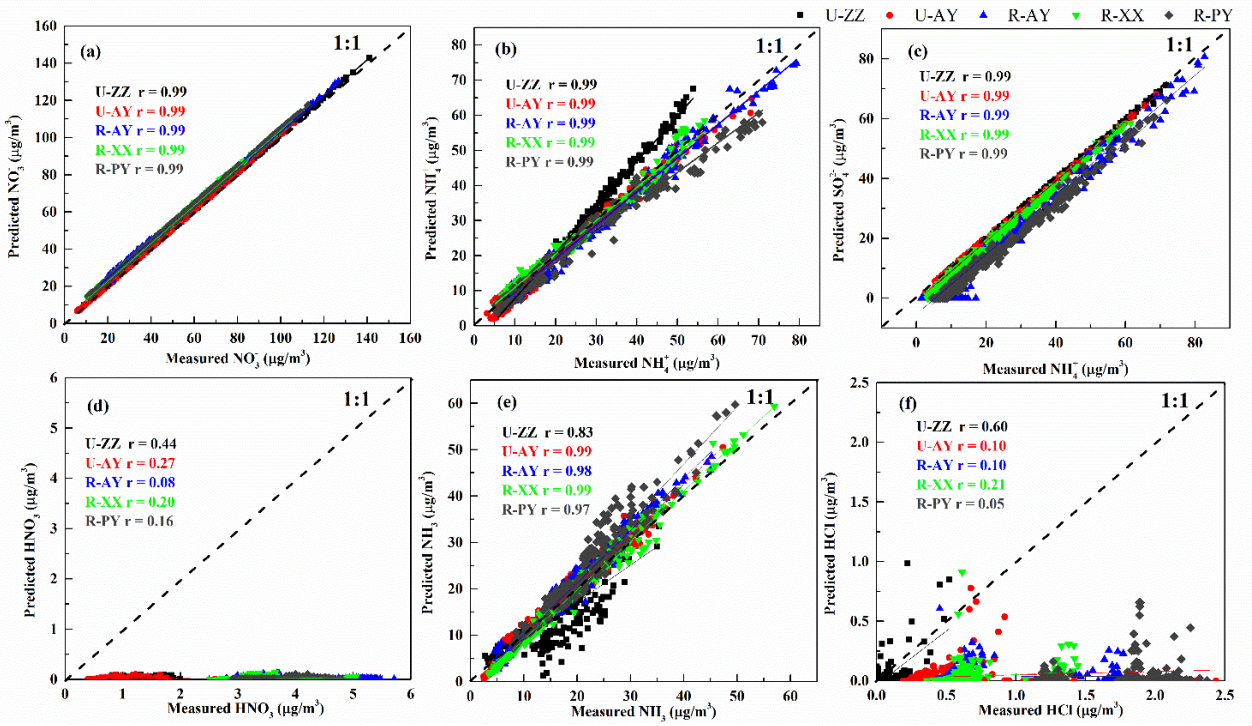

Fig. S2 Comparisons of predicted and measured NH_4^+, SO_4^{2-}, NO_3^-, NH_3, HNO_3 and HCl at the five sites.

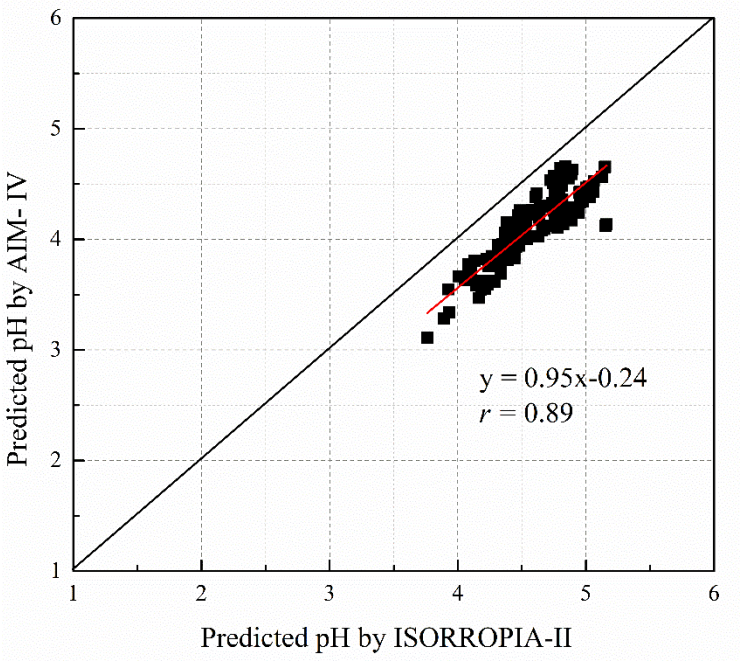

Fig. S3 Comparison of predicted pH by ISORROPIA-II with E-AIM IV at U-ZZ site.

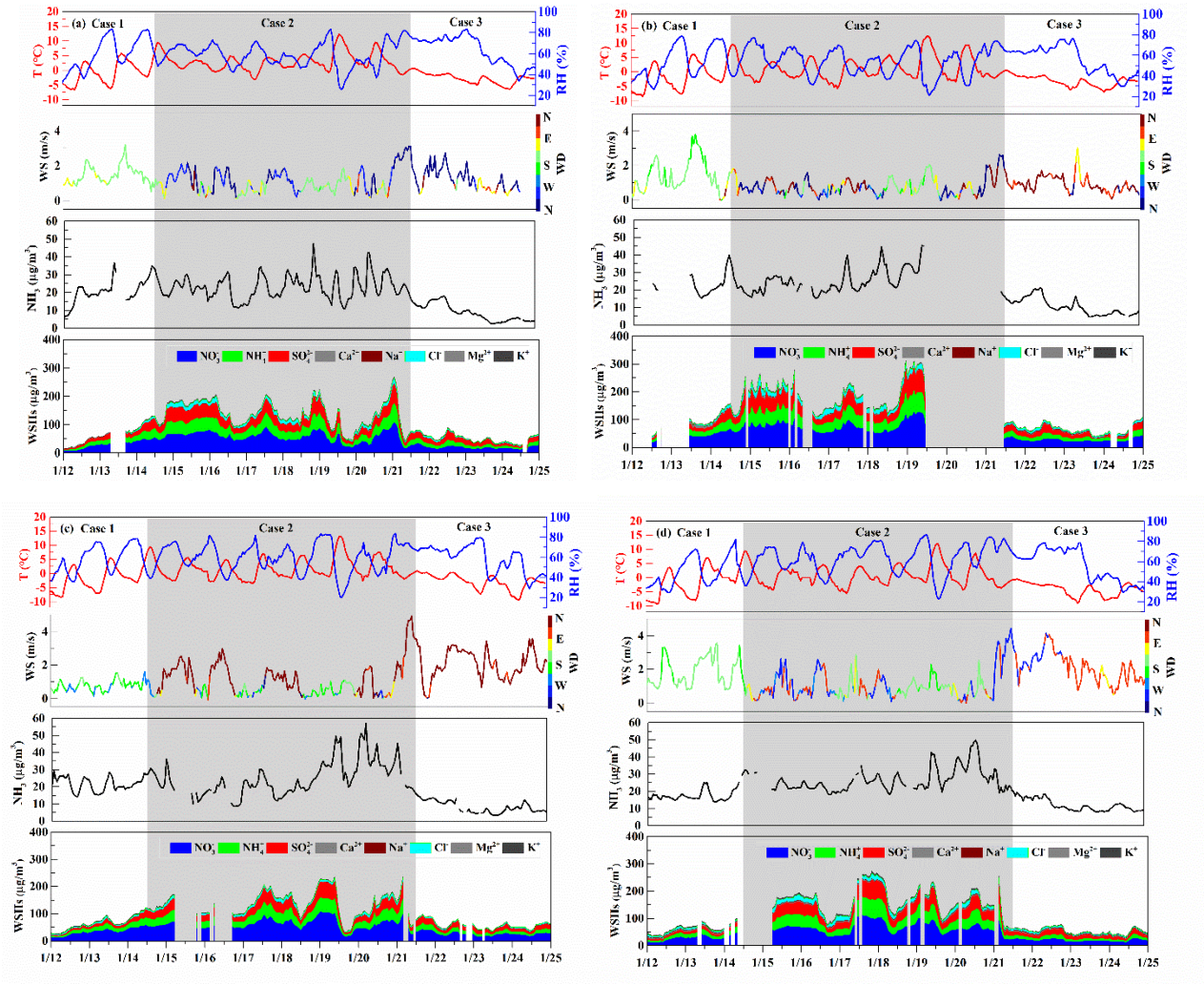

Fig. S4 Fig. 2 Temporal variations of temperature (T), relative humidity (RH), wind speed (WS), wind direction (WD), and concentrations of NH_3 and water-soluble inorganic ions (WSIIs) in three cases at U-AY (a), R-AY (b), R-XX (c), and R-PY (d) sites.

.

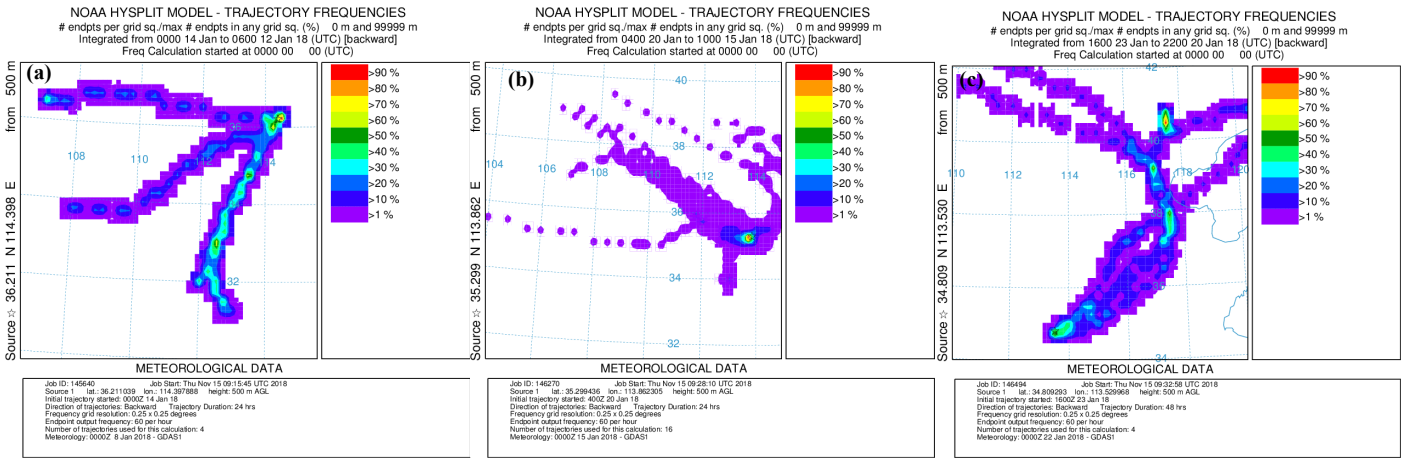

Fig. S5 Trajectory frequencies of typical periods in Cases 1 (a), 2(b), and 3 (c).

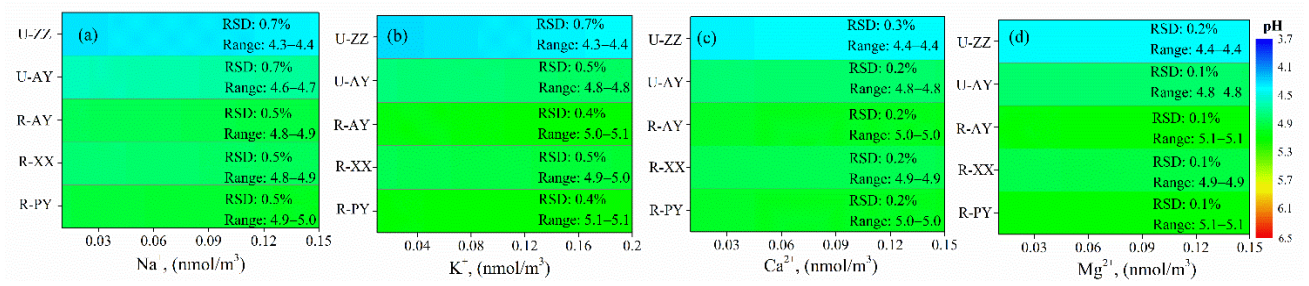

Fig. S6 Sensitivity tests of $PM_{2.5}$ pH to Na^+, K^+, Ca^{2+} and Mg^{2+} in Case 2. The color scale bar represents the pH values. The relative standard deviation (RSD) and range (Range) represent the variation degree and range of pH values in the test.

89 Table S1 Summarized of NH_3 concentrations ($\mu g/m^3$) in this study and other sites.

Cities	Period	NH_3	References
Zhengzhou, China	2018.01	22.0 ±8.9	This study
Anyang, China	2018.01	25.3 ± 10.5	This study
Anyang, China	2018.01	25.8 ± 12.0	This study
Xinxiang, China	2018.01	26.1 ± 14.0	This study
Puyang, China	2018.01	27.1 ± 17.3	This study
Zhengzhou, China	2017.03–2018.04	11.7	Wang et al., 2018
Beijing, China	2015.01–03	7.3	Zhang et al., 2018
Beijing, China	2008.02–2010.07	22.8 ± 16.3	Wang et al., 2018
Beijing, China	2007.01–2010.07	10.2 ± 10.8	Wang et al., 2018
Beijing, China	2001.07–2001.08	16.8–42.2	Wang et al., 2018
North China Plain, China	2006.08–2009.09	11.7–31.9	Shen et al., 2011
Xi'an, China	2006.04–2007.04	18.6	Wang et al., 2018
Xi'an, China	2006.04–2007.04	20.3	Wang et al., 2018
Chengdu, China	2014.07–2015.04	10.5 ± 4.8	Wang et al., 2016
Wanzhou, China	2014.07–2015.04	8.3 ± 4.7	Wang et al., 2016
shanghai, China	2014.05–2015.06	7.8	Chang et al., 2019
Hangzhou, China	2012.04–05	12.8	Jansen et al., 2014
Dalian, China	2010.09–2012.04	1.5	Luo et al., 2014
Fenghua, China	2010.08–2012.05	3.7	Luo et al., 2014
Fujian, China	2015.06–2016.05	21.0 ± 7.9	Wang et al., 2018
Fujian, China	2015.06–2017.03	10.5–13.5	Wu et al., 2018
Hong Kong, China	2003.10–2006.05	10.2	Tanner, 2009
Carolina, USA	2000.01–12	0.4–3.4	Walker et al., 2004
Delhi, India	2013.01–2015.12	25.3 ± 4.6	Saraswati et al., 2019

90

Table S2 Pearson's correlation coefficients (r) between H^+_{air} and input data at the five sites.

	TNH_x	SO_4^{2-}	TNO_3	TCl	K^+	Ca^{2+}	Na^+	Mg^{2+}	T	RH
U−ZZ	0.650**	0.867**	0.828**	0.430**	0.757**	−0.161*	0.306**	−0.009	0.000	0.337**
U−AY	0.368**	0.625**	0.458**	0.406**	0.388**	−0.234**	−0.095	−0.027	0.045	0.610**
R−AY	0.544**	0.765**	0.607**	0.602**	0.551**	−0.137*	0.098	−0.018	−0.138*	0.631**
R−XX	0.301**	0.638**	0.502**	0.223**	0.138*	−0.248**	0.103	−0.050	−0.023	0.637**
R−PY	0.703**	0.811**	0.767**	0.419**	0.485**	0.060	−0.138*	0.026	0.146*	0.658**

* Correlation is significant at the 0.05 level (two-tailed).

** Correlation is significant at the 0.01 level (two-tailed).

References:

Chang, Y., Zou, Z., Zhang, Y., Deng, C., Hu, J., Shi, Z., Dore, A. J., Collett, J. L.: Assessing contributions of agricultural and nonagricultural emissions to atmospheric ammonia in a Chinese megacity. Environ. Sci. Technol., 53, 1822–1833, 2019.

Jansen, R. C., Shi, Y., Chen, J., Hu, Y., Xu, C., Hong, S., Li, J., Zhang, M.: Using hourly measurements to explore the role of secondary inorganic aerosol in $PM_{2.5}$ during haze and fog in Hangzhou, China. Adv. Atmos. Sci., 31, 1427–1434, 2014.

Luo, X. S., Tang, A. H., Shi, K., Wu, L. H., Li, W. Q., Shi, W. Q., Shi, X. K., Erisman, J. W., Zhang, F., Liu, X. J.: Chinese coastal seas are facing heavy atmospheric nitrogen deposition. Environ. Res. Lett., 9, 095007, 2014.

Saraswati, Sharma, S. K., Saxena, M., Mandal, T. K.: Characteristics of gaseous and particulate ammonia and their role in the formation of secondary inorganic particulate matter at Delhi, India.

Atmos. Res., 218, 34–49, 2019.

Shen, J., Liu, X., Ying, Z., Fangmeier, A., Goulding, K., Zhang, F.: Atmospheric ammonia and particulate ammonium from agricultural sources in the North China Plain. Atmos. Environ., 45, 5033–5041, 2011.

Tanner, P.A.: Vehicle-related ammonia emissions in Hong Kong. Environ. Chemi. Lett., 7, 37–40, 2009.

Walker, J. T., Whitall, D. R., Robarge, W. P., Paerl, H. W.: Ambient ammonia and ammonium aerosol across a region of variable ammonia emission density. Atmos. Environ., 38, 1235–1246, 2004.

Wang, C., Yin, S., Bai, L., Zhang, X., Gu, X., Zhang, H., Lu, Q., Zhang, R.: High-resolution ammonia emission inventories with comprehensive analysis and evaluation in Henan, China, 2006–2016. Atmos. Environ., 193, 11–23, 2018.

Wang, H., Yang, F., Shi, G., Tian, M., Zhang, L., Zhang, L., Fu, C.: Ambient concentration and dry deposition of major inorganic nitrogen species at two urban sites in Sichuan Basin, China. Environ. Pollut., 219, 235–244, 2016.

Wu, S., Dai, L., Wei, Y., Zhu, H., Zhang, Y., Schwab, J. J., Yuan, C.: Atmospheric ammonia measurements along the coastal lines of Southeastern China: Implications for inorganic nitrogen deposition to coastal waters. Atmos. Environ., 177, 1–11, 2018.

Zhang, R., Sun, X., Huang, Y., Shi, A., Yan, J., Nie, T., Yan, X., Li, X.: Secondary inorganic aerosols formation during haze episodes at an urban site in Beijing, China. Atmos. Environ., 177, 275–282, 2018.